ROMAI J., v.11, no.1(2015), 47–67

NUMERICAL EVALUATION OF CONCRETE-FACED ROCKFILL DAM UPON MULTIPLANE DAMAGE MODEL

Mohsen Ghadrdan, Seyed A. Sadrnejad, Tahereh Shaghaghi, Kazem Ghasimi
Faculty of Civil Engineering, K.N.Toosi University of Technology, Tehran, Iran
mq1365@gmail.com, sadrnejad@kntu.ac.ir, tahereh.shaghaghi@gmail.com, kazem.ghasimy@gmail.com

Abstract This paper proposed multiplane framework as a new approach to study the interaction of different materials. The Five identified types of damage (cracks) upon damage functions are employed in a simple multiplane framework to predict the damaged behavior and its nonlinear effects on materials as well as their interactions. The obtained results show a good match with experimental tests.

As a case study, a high concrete-faced rockfill dam (CFRD) is numerically investigated. Cracks and damage prone areas of concrete layer are examined in details. Accordingly, seepage control upon crack effects of concrete face permeability can be evaluated and considered.

Keywords: multiplane, damage function, concrete-faced rockfill dam, interaction, crack.
2010 MSC: 97U99.

1. INTRODUCTION

High CFR dams have been the center of attention over the few past decades owing to their benefits such as fast and less costly construction as well as their flexible design for different topography [1]. Despite the many advantages to this type of dam, the lack of accurate information about the behavior of CFRD, particularly its concrete slab in different loading conditions, is a critical problem for engineering [2, 3, 4, 5, 6, 7]. The interaction created between concrete slabs and cushion layer determines the response of concrete slab during different loading conditions. This interaction is a result of different stiffness of these two parts of CFR dam. The separation of concrete slabs from cushion layer is due to different settlement or deformation of dam body and concrete slabs. This separation is more important in high CFR dams because of its increasing in stress level [8].

As the concrete is not a flexible material, the separation of concrete from rockfill body and its deformation can produce and propagate cracks in the concrete slabs. Cracks can have an adverse impact on the impermeability of concrete slabs, posing threat to the safety of dam.

Various numerical methods have been proposed to investigate the interaction between soil and structure. The methods can be categorized into three main approaches. The first approach treats the interface as an ideal material [9]. This approach is easy to

be implemented numerically and analytically. The simplification used in this method leads to the omission of some important details and effects of interface. The second approach is based on contact mechanics, e.g., Lagrange methods and penalty function methods [8]. It is difficult to develop a model for predicting accurate behavior of interface using the contact mechanic approach. The third approach is interface element which is based on continuum numerical methods by using various constitutive models [8, 9]. Interface element is widely used for describing the interaction between different media [10, 11, 12, 13, 14, 15]. Mohr-Coulomb strength criteria, the Clough-Duncan model and the ideal elasto-plasticity model are often used for such interfaces [16, 17, 18].

To study the interaction between materials, two aspects need to be considered: an accurate constitutive model and an effective numerical solution.

In this paper, a multiplane framework and a damage function as a constitutive model have been used to model the interaction between concrete slabs and cushion layer as interface elements. The damage function and the multiplane framework are also assigned to concrete and rockfill materials. This approach is capable of predicting the behavior of materials under any arbitrary stress-strain path and final failure mechanism. By using the multiplane framework, the inherent anisotropy of materials is considered.

By implementing multiplane framework into FEM software, a three-dimensional CFR dam is analyzed. Valid experimental tests are used for confirming the multiplane framework and damage function. Finally, a critical point of concrete slab and the orientation of predicted cracks propagation have been discussed in details.

2. MODELING APPROACH

2.1. BACKGROUND OF THE MULTIPLANE FRAMEWORK

The continuous models are commonly categorized as macroscopic models and mesoscopic models. The macroscopic models consist of damage or plasticity theory or a combination of both; and the mesoscopic models include such models as multilaminate or microplane models. The difference between these two groups is in dealing with the definition of the relation between stress and strain tensors [19].

The basic concept of multilaminate approach is by considering the relation between strain and stress tensors can be assembled from the planes with different orientations. The formulation of this idea was developed later. Initially, this idea was used as a constitutive model for metal and was known as a “Slip theory” [20] . This theory was based on the assumption that slip in any particular orientation leads to a plastic shear strain that depends only on the history of the corresponding component of shear stresses/strains. Multilaminate models were adopted for anisotropic rocks, clays and granular materials [21, 22, 23, 24]. The concept was developed by using continuum damage mechanics under the name “microplane” [25]. The mechanical

behavior of quasi brittle materials has been model with microplane theory [26, 27, 28, 29, 30].

2.2. MULTIPLANE FORMULATION WITH KINEMATIC CONSTRAINT

Multilaminate theories were based on static constraint approach. In the static constraint approach, the macroscopic stress tensor in the center of the unit sphere was projected on the oriented microscopic planes which are tangent on the surface of the sphere in the prescribed points. Micro strains were calculated by constitutive laws introduced on the micro planes. Macro strain tensor was obtained from superposition of micro strains of each plane [24, 31, 32, 33]. In the static constraint approach, the equilibrium of the forces are automatically satisfied in the point but the superposition of micro strain components, does not guarantee the correct macro strain tensor.

In the microplane theory, kinematic constraint was employed by projecting strain tensor instead of stress tensor on the planes. In this condition, the problem of compatibility was solved but equilibrium condition was not satisfied.

Number of planes used by previous studies was 13 which could not satisfy superposition effect and some data of strain had been omitted [21, 26, 34, 35, 36, 37]. In this paper the number of planes is modified to overcome some deficiencies of this approach and presents "multiplane" model. By considering three perpendicular planes in 13 previous positions 39 planes established in such a way that one of them is tangential to sphere. By eliminating extra surfaces because of symmetry of sphere and orientations, 17 planes were obtained. Better prediction of strain induced anisotropy achieved by using 17 planes instead of 13 planes [32]. The unite sphere of multiplane model includes of 34 planes tangent to the sphere's surface (Fig. 1). The specifications of 17 planes are listed in Table 1.

Because volumetric strains do not depend on orientation, volumetric and deviatoric strains are separated from each other in the macroscopic strain and only deviatoric strains project on the planes.

The orientation of each plane is characterized by the unite normal to the plane with components of n_i , i=1, 2, 3 (any subscript refers to the components in Cartesian coordinate axis x_i). In order to characterize the shear strain on the planes, it is required to define two extra coordinate directions M and L which indicate two orthogonal unite coordinate vectors m_i and l_i, respectively (Fig. 2). The unit coordinate vector $\vec{m}$ is chosen and $\vec{l}$ could be obtained as $\vec{l} = \vec{m} \times \vec{n}$.

By projecting macroscopic strain tensor (ϵ_{ij}) on each plane, three components of microscopic strains yield which one is normal (ϵ_N) and two of them are tangential (ϵ_L, ϵ_M). Microscopic components of strain projected on each plane are yielded as following relations:

$$N_{ij} = n_i n_j, \tag{1}$$

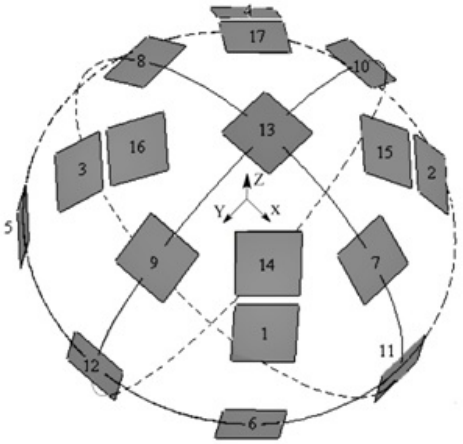

Fig. 1.: Position of 17 integration points on the unite sphere surface.

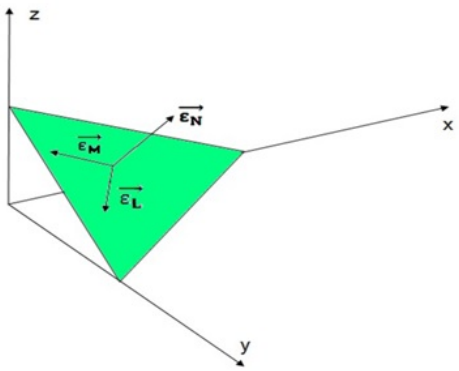

Fig. 2.: Strain components on a plane.

Table 1: Planes normal vectors and weights.

Number of Plane	l_i	m_i	n_i	w_i
1	$\frac{\sqrt{3}}{3}$	$\frac{\sqrt{3}}{3}$	$\frac{\sqrt{3}}{3}$	0.020277985
2	$\frac{\sqrt{3}}{3}$	$-\frac{\sqrt{3}}{3}$	$\frac{\sqrt{3}}{3}$	0.020277985
3	$-\frac{\sqrt{3}}{3}$	$\frac{\sqrt{3}}{3}$	$\frac{\sqrt{3}}{3}$	0.020277985
4	$-\frac{\sqrt{3}}{3}$	$-\frac{\sqrt{3}}{3}$	$\frac{\sqrt{3}}{3}$	0.020277985
5	$\frac{\sqrt{2}}{2}$	$\frac{\sqrt{2}}{2}$	0	0.058130468
6	$-\frac{\sqrt{2}}{2}$	$\frac{\sqrt{2}}{2}$	0	0.058130468
7	$\frac{\sqrt{2}}{2}$	0	$\frac{\sqrt{2}}{2}$	0.030091134
8	$-\frac{\sqrt{2}}{2}$	0	$\frac{\sqrt{2}}{2}$	0.030091134
9	0	$-\frac{\sqrt{2}}{2}$	$\frac{\sqrt{2}}{2}$	0.030091134
10	0	$\frac{\sqrt{2}}{2}$	$\frac{\sqrt{2}}{2}$	0.030091134
11	1	0	0	0.038296881
12	0	1	0	0.038296881
13	0	0	1	0.02030006
14	$\frac{1}{\sqrt{6}}$	$\frac{1}{\sqrt{6}}$	$\sqrt{\frac{2}{3}}$	0.019070616
15	$\frac{1}{\sqrt{6}}$	$-\frac{1}{\sqrt{6}}$	$\sqrt{\frac{2}{3}}$	0.019070616
16	$-\frac{1}{\sqrt{6}}$	$\frac{1}{\sqrt{6}}$	$\sqrt{\frac{2}{3}}$	0.019070616
17	$-\frac{1}{\sqrt{6}}$	$-\frac{1}{\sqrt{6}}$	$\sqrt{\frac{2}{3}}$	0.019070616

$$\epsilon_N = N_{ij}\epsilon_{ij}, \tag{2}$$

$$M_{ij} = \frac{m_i n_j + m_j n_i}{2}, \tag{3}$$

$$\epsilon_M = M_{ij}\epsilon_{ij}, \tag{4}$$

$$L_{ij} = \frac{l_i n_j + l_j n_i}{2}, \tag{5}$$

$$\epsilon_L = L_{ij}\epsilon_{ij}, \tag{6}$$

$$\sigma_{ij} = \sigma_V \delta_{ij} + \frac{3}{2\pi}\int [\sigma_N (N_{ij} - \frac{\delta_{ij}}{3}) + \sigma_L L_{ij} + \sigma_M M_{ij}] d\Omega. \tag{7}$$

Where repeated indicates imply summation over i =1, 2, 3. By applying convenient constitutive law, micro stress can be updateable and by employing principle of virtual work, the relation between micro stress and macro stress tensor could yield as follows [27].

Where Ω is the surface of a unit hemisphere; δ_{ij} is the Kronecker delta; σ_V is the volumetric part of stress, σ_N is the normal micro stress and σ_L and σ_M represent the shear stresses on the planes. By using a finite number of integration points on the surface of the hemisphere and applying Gaussian integration, below equilibrium is derived [27]:

$$\sigma_{ij} = \sigma_V \delta_{ij} + \frac{3}{2\pi}\int_\Omega S_{ij} d\Omega \simeq \sigma_V \delta_{ij} + 6\sum_{\mu=1}^{N_m} w_\mu S_{ij}^{(\mu)}, \tag{8}$$

$$S_{ij} = \sigma_D (N_{ij} - \frac{\delta_{ij}}{3}) + \sigma_L L_{ij} + \sigma_M M_{ij}, \tag{9}$$

where N_m and w_μ are the number of integration points on the hemisphere and the weight of each planes, respectively.

The deviatoric part of the constitutive matrices is computed from the superposition of its counterparts on the microplanes. Such counterparts are, in turn, calculated according to the types of damage that occur on each plane. Macroscopic constitutive matrix consists of deviatoric and volumetric parts and is obtained as follows:

$$D_i jkl = \frac{3}{4\pi}\int_\Omega (\frac{E}{1+v})[(N_{ij} - \frac{\delta_{ij}}{3})(N_{kl} - \frac{\delta_{kl}}{3}) + M_{ij}M_{kl} + L_{ij}L_{kl}] d\Omega + \frac{E}{1-2v}\frac{\delta_{kl}}{3}\delta_{ij}. \tag{10}$$

Where E and v represent the elastic modulus and Poisson's coefficient, respectively. As can be seen, the formulation of this approach is based on two basic material parameters which are Elasticity and Poission's coefficient.

2.3. FORMULATION OF ANISOTROPY DAMAGE FUNCTION

Multiplane framework cannot predict the behavior of materials independently. It is used in the form of a constitutive law. The computational sequence multiplane damage model is shown in Fig. 3.

Each plane, because of its different condition of loading, encounters different damage. By using the superposition of counterparts on the planes the deviatoric part of the constitutive matrix is computed. By considering five types of loading conditions, five damage functions are applied as follows:
- Hydrostatic compression,
- Hydrostatic extension,
- Pure shear,
- Shear + compression,
- Shear + extension.

Each plane may encounter one of the five mentioned basic loading conditions at each time of loading. For each state of plane loading, one of the five damage functions is computed with respect to the history of micro stress/strain components [31]. No damage is considered for hydrostatic compression. For other conditions of loading the damage function can be written as:

$$\epsilon_{eq} \leq a \rightarrow \omega = 0, \tag{11}$$

$$\epsilon_{eq} > a \rightarrow \omega = 1 - \frac{a}{\epsilon_{eq}} \times exp[-(\frac{\epsilon_{eq} - a}{b - a})], \tag{12}$$

where ϵ_{eq} equals the magnitude of projected deviatoric strain vector on each plane, and w is the damage value; "a" and "b" are the damage function parameters and can be obtained from experimental data and experiences. Damage get started when ϵ_{eq} reaches to "a" value and "b" is a parameter for controlling gradient of softening.

2.4. NUMERICAL FORMAT OF INTERACTION MODEL

In this paper, an interface element with approach of multiplane framework is employing for simulating interaction between concrete layer and rockfill. By using multiplane concept sliding, separation/closing of interaction of intact parts could be derive as the result of sliding, separation/closing surrounding boundary planes. It could be possible just by considering relative planes to the interface.

The damage function of planes for pure shear loading condition used parameters which are calibrated by a shear interface test of Zipingpu CFRD. No strength is considered for the planes which are in tension condition of loading.

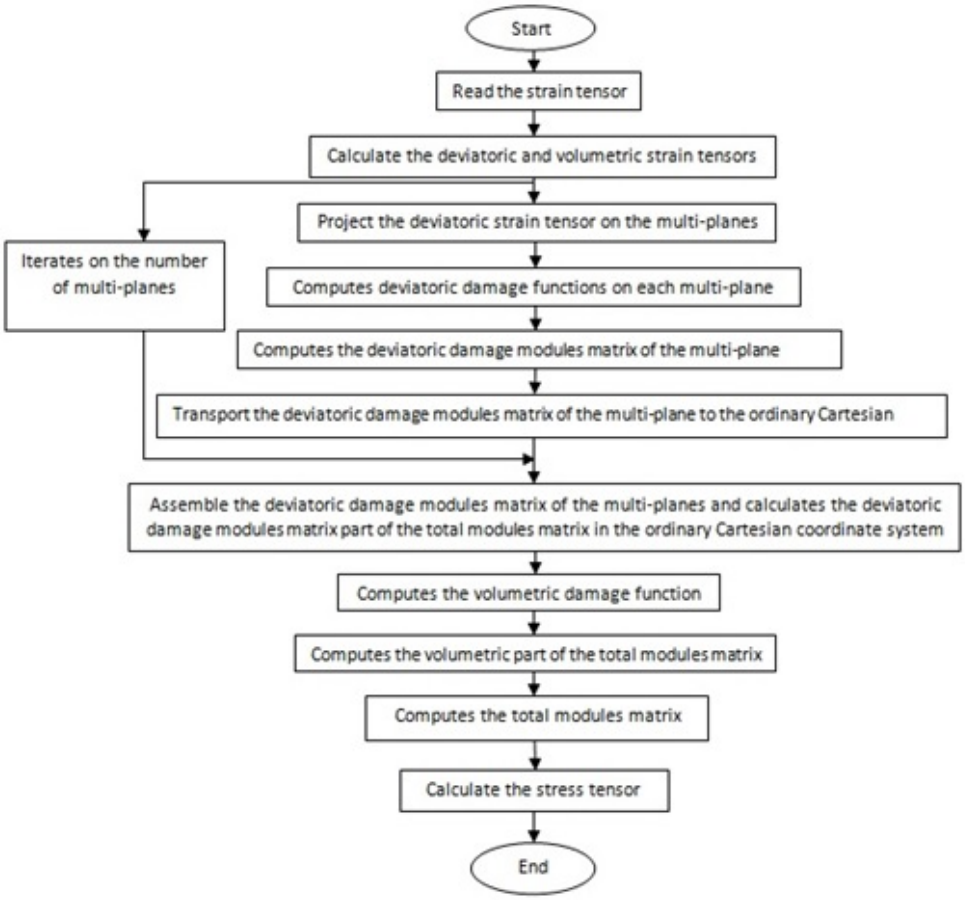

Fig. 3.: The procedure of proposed multiplane damage model in each increment of analyzing.

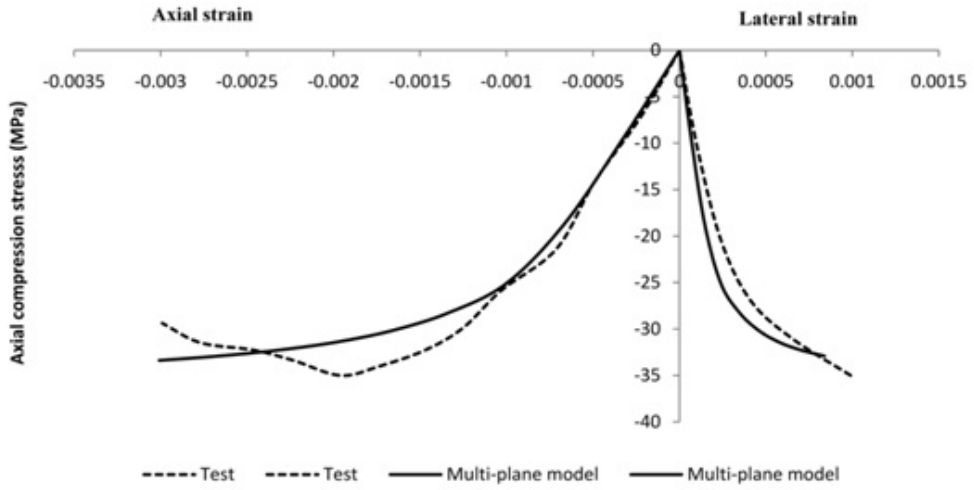

Fig. 4.: Results of uniaxial compression test of concrete obtained by proposed microplane damage model.

3. CORRELATION STUDIES

Because well-documented test results were not available for the concrete and rockfill materials of the Zipingpu, tests results on the concrete and rockfill materials from [38, 39] are used to calibrate the materials model in this study.

3.1. UNIAXIAL COMPRESSION TEST

A uniaxial compression test of concrete is used for evaluating the validity of the model. As can be seen in the Fig. 4, there is a good agreement between the model prediction results and the experimental evidences [38]. The Young modulus of concrete was considered 35 GPa and poison ratio was 0.2.

Because the uniaxial load is applied in Z orientation, the plane 13 is under compressive normal stress and no shear stress is achieved. The loading of the plane 13 is hydrostatic compression and no damage is seen on the plane 13. It is notable that, normal micro stress on the plane 13 reaches 47 MPa with -0.00189 micro strain. However, for showing other planes clearly we omit this undamaged plane in Fig. 5. Planes number 5, 6, 11 and 12 experience only tensile stress because of normal orientation of these planes to the load direction on the unit sphere (Fig. 5). Planes 1, 2, 3, 4, 7, 8, 9, 10, 14, 15, 16 and 17 include tangential and normal streses (Fig. 5 and Fig. 6). The growth of damage function values on the planes during the test are shown in Fig. 7.

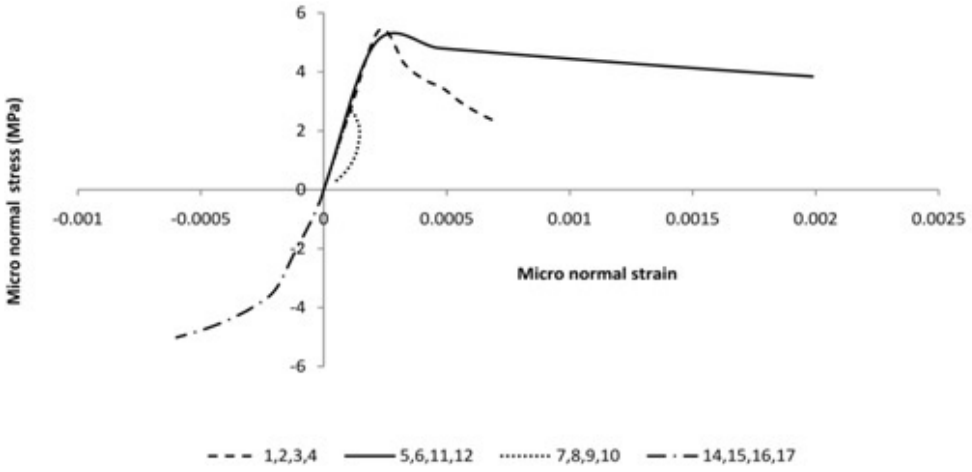

Fig. 5.: Variation of micro components of normal strain and stress on planes during uniaxial compression concrete test.

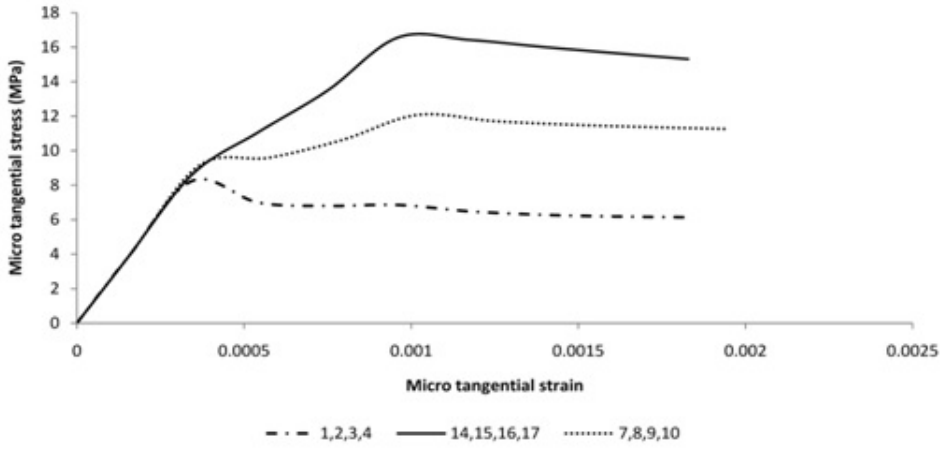

Fig. 6.: Variation of micro components of tangential strain and stress on planes during uniaxial compression concrete test.

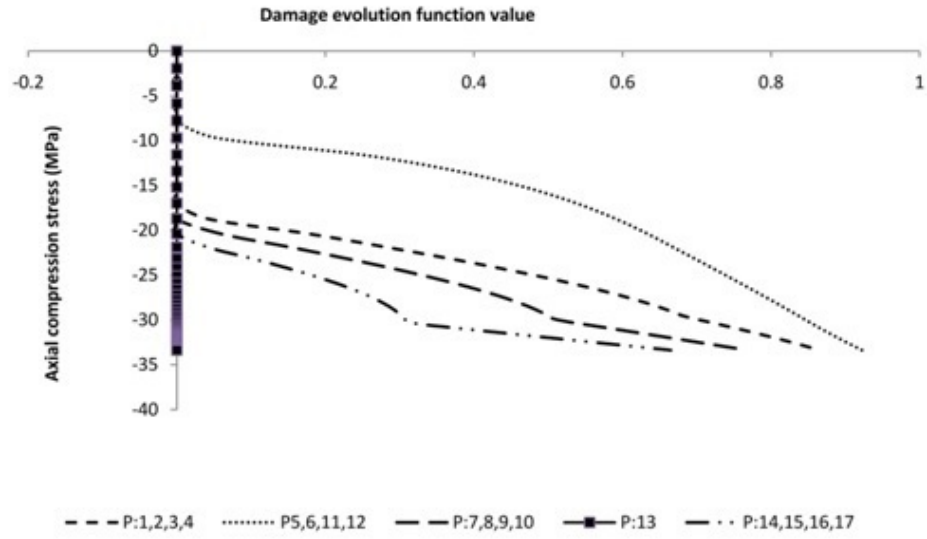

Fig. 7.: Comparison of damage evolution functions on the planes during uniaxial compressive loading.

3.2. TRIAXIAL COMPRESSION TEST

A triaxial compressive test of limestone rockfill material [39] which has 700 KPa confining pressure is used for correlation rockfill materials of the CFR dam. A good match is derived between the laboratory results and the proposed model predictions in the macroscopic scale (Fig. 8). The Young modulus and poison ratio of rockfill materials were 230 MPa and 0.25 respectively.

Because no tensile strength is considered for rockfill material, planes 5, 6, 11 and 12 are not capable to tolerate tensile stresses (Fig. 9 and Fig. 10). No damage and no tangential stress are resulted for plane 13 in triaxial test. Micro stress of plane 13 is reached to 6989 KPa while micro strain is reached to -0.03798. The damage values during the test are shown in Fig. 11.

4. APPLICATION

Zipingpu CFRD is one of the largest CFRDs in China with 156m height. The dam was completed in 2006 and represented the latest CFRD technology in China. The valley is unsymmetrical V shape and the normal water level storage is 873.5m (Fig. 16).

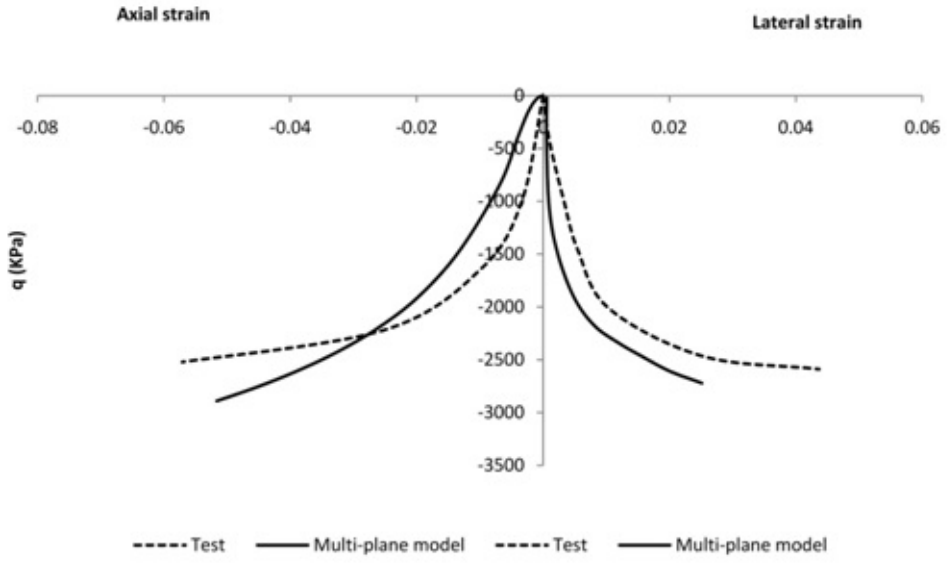

Fig. 8.: Results of trixial compression test of rockfill obtained by proposed microplane damage model.

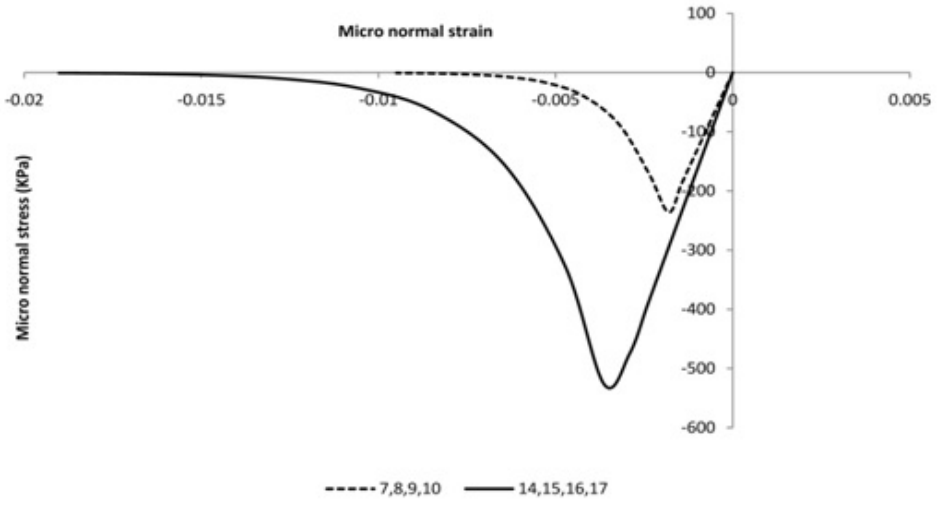

Fig. 9.: Variation of micro components of normal strain and stress on planes during triaxial compression rockfill test.

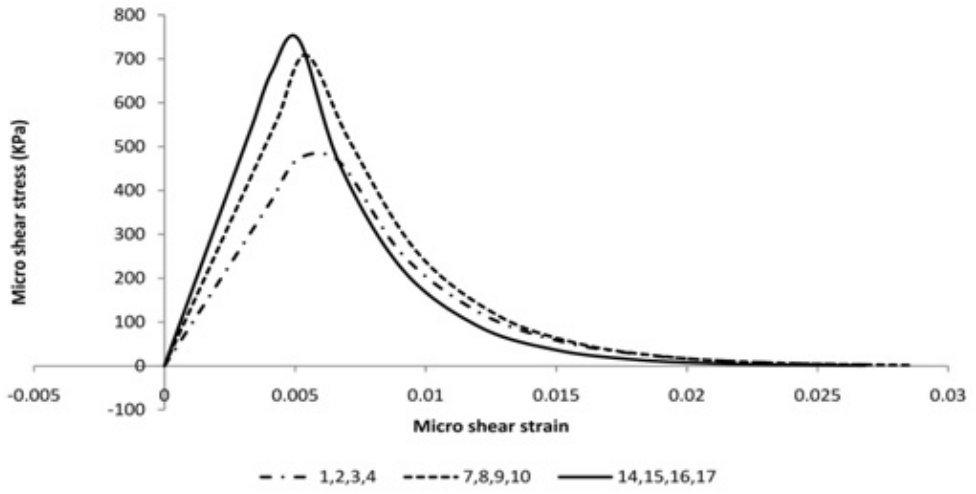

Fig. 10.: Variation of micro components of tangential strain and stress on planes during triaxial compression rockfill test.

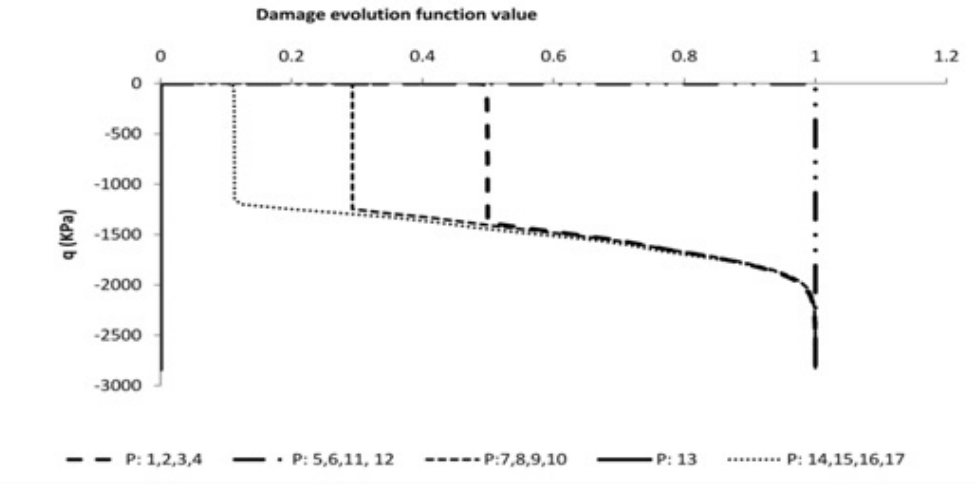

Fig. 11.: Comparison of the damage evolution functions on the planes during triaxial compressive loading.

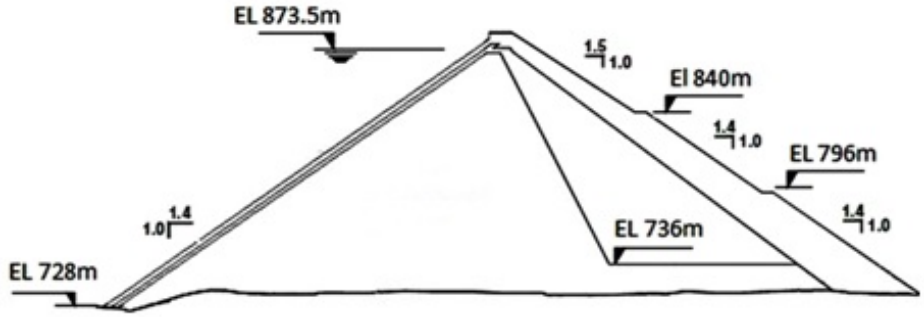

Fig. 12.: Maximum Section of Zipingpu CFRD.

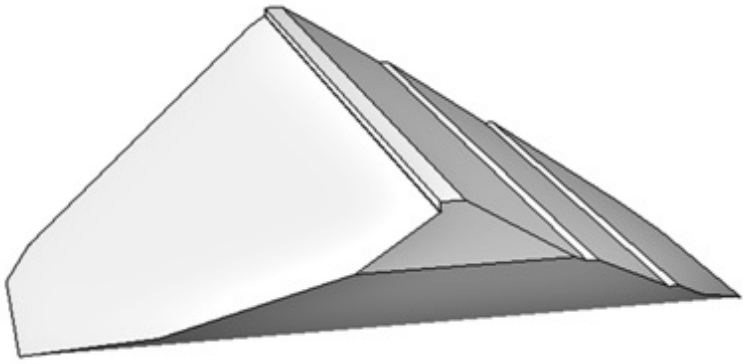

Fig. 13.: Three-dimensional mesh of Zipingpu CFRD.

4.1. FINITE ELEMENT MODEL

Zipingpu CFRD is analyzed using the three-dimensional FEM (Fig. 13). As constitutive model, damage functions are specified to the planes of multiplane framework. The parameters of five damage functions specified to the planes are calibrated and assigned to different parts of CFR dam. Loads are applied gradually and water load is considered as hydrostatic pressure on the concrete layer.

4.2. RESPONSE OF ZIPINGPU CFR DAML

The main deformations of CFRDs occur after construction and initial impounding [40, 41, 42, 43] so the state of stresses after these periods are necessary. The contour lines of vertical stress before and after impounding are shown in the maximum cross section of dam (Fig. 14 and 15). From the results it is seen that, the maximum

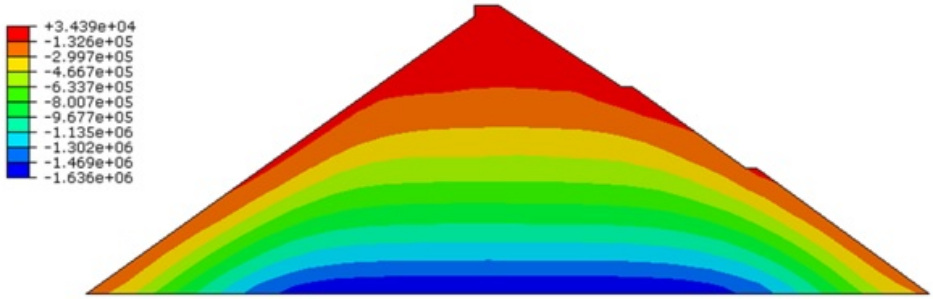

Fig. 14.: Vertical stress contour lines of rockfill body after construction (Pa).

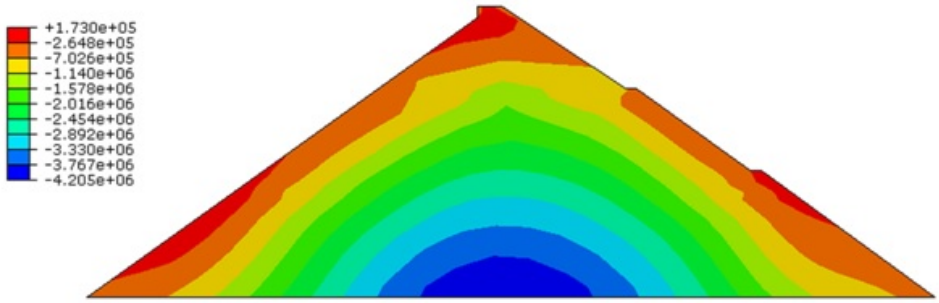

Fig. 15.: Vertical stress contour lines of rockfill body after impunding (Pa).

stress occurred in the middle of base and impounding reservoir changes the states of stresses.

Concrete and rockfill are two materials with different properties. So, their responses to loads are different from each other. Different deformation of these two materials leads to manifestation of prone crack area for sepration of concrete slabs from cushion layer of CFR dam. Contour lines of horizontal stress before and after impounding on the concrete slabs are shown in Fig. 16 and Fig. 17. After the dam was completed, the top elements of slabs exhibited separation (Fig. 16). Due to applying hydrostatic water pressure, compressive region spreads and helps in decrease separation area (Fig. 17).

Responses of concrete slabs are directly effected by micro stress and micro strain path of planes in the concrete. For more detail, a critical point is located on the top of concrete slab at the left corner of dam in the height of 103m is studied. Some of the planes have not suffered any damage during different loadings (planes 2, 4, 5, 6, 9, 11, 15 and 17 after construction and planes 4, 5, 6, 8, 9, 11, 12 and 17 after impounding).

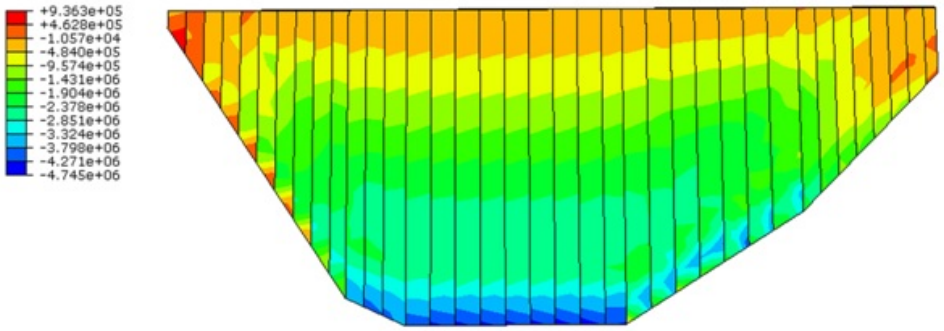

Fig. 16.: Horizontal stress contour lines ofconcrete slabs after construction (Pa).

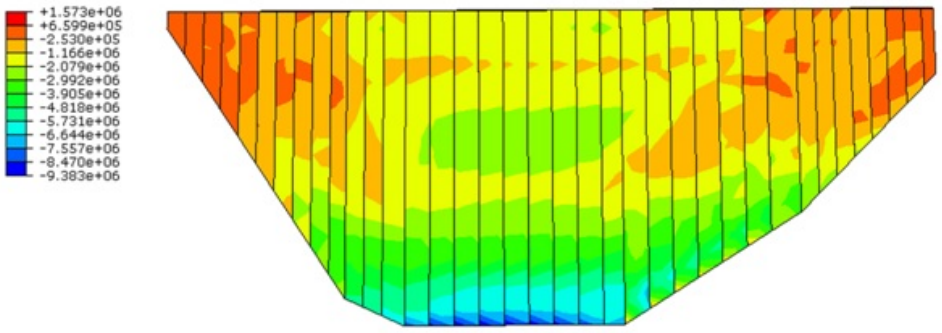

Fig. 17.: Horizontal stress contour lines of slabs after impounding (Pa).

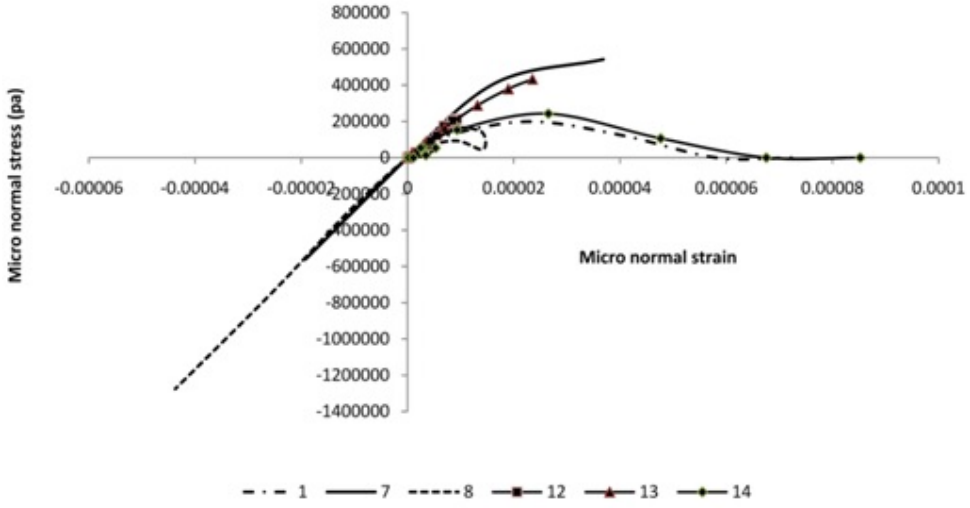

Fig. 18.: Normal stress and strain of planes during construction.

After construction, the damage value function of planes 1, 3, 10, 14 and 16 reach to one. By impounding, planes 1, 2, 3,7, 10, 14, 15 and 16 experience one value of damage function. Both strength and stiffness of these planes decline and planes have not resistance to tolerate stress. Consequently cracks occurred and the directions of cracks are related to the characteristics of the planes.

Variations of micro stress/strain of other planes, during construction (Fig. 18 and Fig. 19) and impounding (Fig. 20 and Fig. 21), are analyzed. Water storage changes stress/strain path of the planes. Damage condition of planes 8 and 12 enhanced and planes 2, 7 and 15 deteriorate by applying water load.

5. CONCLUSION

A new constitutive model for predicting the effects of any arbitrary loading conditions was developed using the approach of a theoretical framework of multiplane and damage functions. Although the proposed model has excellent features, the basis of its formulation is simple and logical and it confers some physical insights that make it convenient to understand. The validity of this approach was verified by experimental tests and good coincident results. By employing multiplane framework and damage functions, the responses of concrete slabs are studied in construction and water storage periods of loading. It is seen that reservoir water has an obvious effect on the response of the concrete slabs. During impounding, some planes unload and some of them heavily load so it makes changes in micro stress/strain. The planes of a critical point of concrete which are more probable to crack, because of having critical dam-

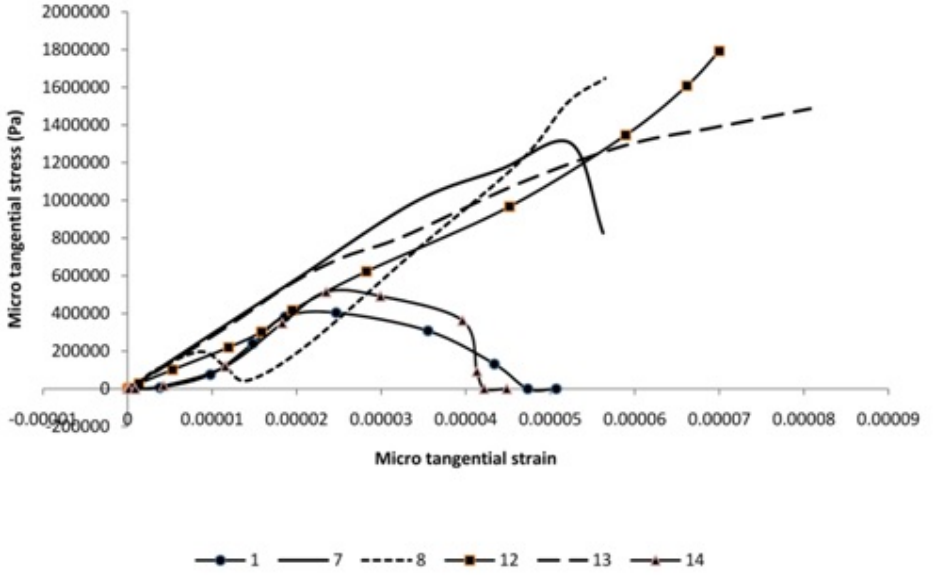

Fig. 19.: Tangential stress and strain of planes during construction.

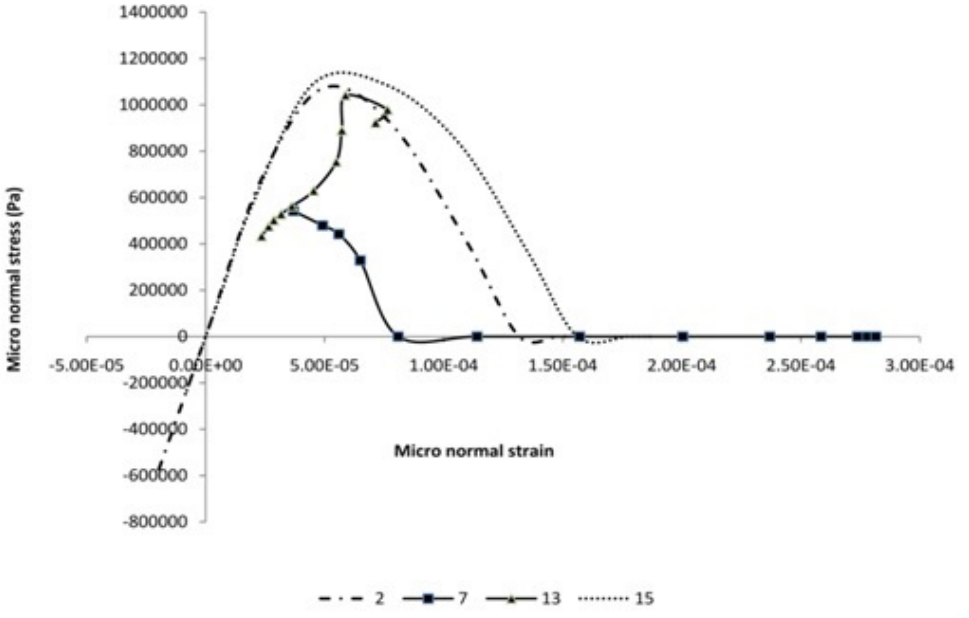

Fig. 20.: Normal stress and strain of planes during impounding.

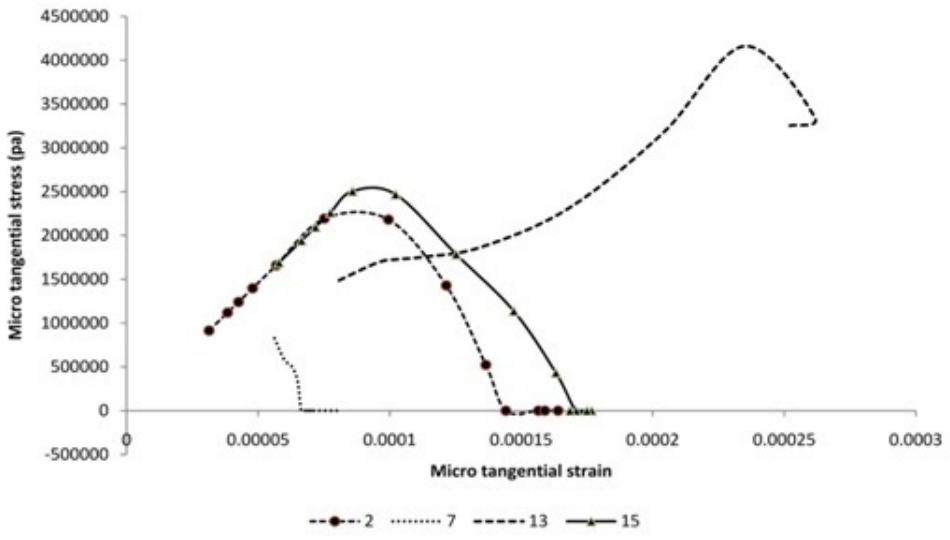

Fig. 21.: Tangential stress and strain of planes during impounding.

age function values, are highlighted. The directions of cracks in the concrete layer can be found by considering damage planes and their orientations.

References

[1] Arici, Y., *Investigation of the cracking of CFRD face plates*, Computers and Geotechnics, **38**, 7(2011), 905-916.

[2] Guros, F., et al., *Seismic design of concrete-faced rockfill dams*, in Proceedings of the 8th World Conference on Earthquake Engineering, San Francisco, 1984.

[3] Priscu, R., *Earthquake engineering for large dams*, 1985.

[4] Seed, H.B., et al., *Seismic design of concrete faced rockfill dams*, in Concrete Face Rockfill Dams-Design, Construction, and Performance, 1985, ASCE.

[5] Sherard, J.L., Cooke, J.B., *Concrete-face rockfill dam: I. assessment*, Journal of geotechnical engineering, **113**, 10(1987), 1096-1112.

[6] Gazetas, G., Dakoulas, P., *Seismic analysis and design of rockfill dams: state-of-the-art*, Soil Dynamics and Earthquake Engineering, **11**, 1(1992), 27-61.

[7] Uddin, N., Gazetas, G., *Dynamic response of concrete-faced rockfill dams to strong seismic excitation*, Journal of geotechnical engineering, **121**, 2(1995), 185-197.

[8] Zhang, B., Wang, J., Shi, R., *Time-dependent deformation in high concrete-faced rockfill dam and separation between concrete face slab and cushion layer*, Computers and Geotechnics, **31**, 7(2004), 559-573.

[9] Zhang, G., Zhang, J.-M., *Numerical modeling of soil-structure interface of a concrete-faced rockfill dam*, Computers and Geotechnics, **36**, 5(2009), 762-772.

[10] Ng, P., Pyrah, I., Anderson, W., *Assessment of three interface elements and modification of the interface element in CRISP90*, Computers and Geotechnics, **21**, 4(1997), 315-339.

[11] Dong, C., *A simple benchmark problem to test frictional contact*, Computer methods in applied mechanics and engineering, **177**, 1(1999), 153-162.

[12] Karabatakis, D., Hatzigogos, T., *Analysis of creep behaviour using interface elements*, Computers and Geotechnics, **29**, 4(2002), 257-277.

[13] Karutz, H., R. Chudoba, Krätzig, W., *Automatic adaptive generation of a coupled finite element/element-free Galerkin discretization*, Finite elements in analysis and design, **38**, 11(2002), 1075-1091.

[14] Oliveira, D.V., LourenĂ§o, P.B., *Implementation and validation of a constitutive model for the cyclic behaviour of interface elements*, Computers and structures, **82**, 17(2004), 1451-1461.

[15] Shakib, H., Fuladgar, A., *Dynamic soil-structure interaction effects on the seismic response of asymmetric buildings*, Soil Dynamics and Earthquake Engineering, **24**, 5(2004), 379-388.

[16] Nam, S. -H. et al., *Seismic analysis of underground reinforced concrete structures considering elasto-plastic interface element with thickness*, Engineering Structures, **28**, 8(2006), 1122-1131.

[17] Zhang, G., Zhang, J.-M., *Constitutive rules of cyclic behavior of interface between structure and gravelly soil*, Mechanics of Materials, **41**, 1(2009), 48-59.

[18] Mahabad, N. M. et al., *Three-dimensional analysis of a concrete-face rockfill dam*, Proceedings of the ICE-Geotechnical Engineering, **167**, 4(2012), 323-343.

[19] Galavi, V., Schweiger, H. F., *Nonlocal multilaminate model for strain softening analysis*, International Journal of Geomechanics, **10**, 1(2010), 30-44.

[20] Batdorf, S.B., Budiansky, B., *A mathematical theory of plasticity based on the concept of slip*, National Advisory Committee for Aeronautics, 1949.

[21] Pande, G.N., Sharma, K. *Multi-laminate model of clays-a numerical evaluation of the influence of rotation of the principal stress axes*, International journal for numerical and analytical methods in geomechanics, **7**, 4(1983), 397-418.

[22] Pietruszczak, S., Pande, G., *Multi-laminate framework of soil models-plasticity formulation*, International Journal for Numerical and Analytical Methods in Geomechanics, **11**, 6(1987), 651-658.

[23] Roosta, R.M., *Rock joint modeling using a visco-plastic multilaminate model at constant normal load condition*, Geotechnical and Geological Engineering, **24**, 5(2006), 1449-1468.

[24] Sadrnejad, S., Pande, G., *A multilaminate model for sands*, in Proc. Int. Symp. Num. Models in Geomech, NUMOG III, 1989.

[25] Bazant, Z.P., Gambarova, P.G., *Crack Shear in Concrete: Crack Band Microflane Model*, Journal of Structural Engineering, **110**, 9(1984), 2015-2035.

[26] Baiarti, Z., *Microplane model for strain-controlled inelastic behaviour*, in Mechanics of Engineering Materials, C. S. Desai, R. H. Gallagher, 1984.

[27] Bazant, Z.P. et al., *Microplane model for concrete: II: data delocalization and verification*, Journal of Engineering Mechanics, **122**, 3(1996), 255-262.

[28] Carol, I., Bazant, Z.P., *Damage and plasticity in microplane theory*, International Journal of Solids and Structures, **34**, 29(1997), 3807-3835.

[29] Brocca, M., Bazant, Z.P., Daniel, I.M., *Microplane model for stiff foams and finite element analysis of sandwich failure by core indentation*, International Journal of Solids and Structures, **38**, 44(2001), 8111-8132.

[30] Brocca, M., L. Brinson, Bazant, Z., *Three-dimensional constitutive model for shape memory alloys based on microplane model*, Journal of the Mechanics and Physics of Solids, **50**, 5(2002), 1051-1077.

[31] Sadrnejad, S., Labibzadeh, M., *A. continuum/discontinuum micro plane damage model for concrete*, International Journal of Civil Engineering, 4, 2006, 296-313.

[32] Ghadrdan, M., S.A. Sadrnejad, T. Shaghaghi, *Numerical evaluation of geomaterials behavior upon multiplane damage model*, Computers and Geotechnics, 68, 2015, 1-7.

[33] Zienkiewicz, O., Pande, G., *Time-dependent multilaminate model of rocks-a numerical study of deformation and failure of rock masses*, International Journal for Numerical and Analytical Methods in Geomechanics, 1977. 1(3): p. 219-247.

[34] Khosroshahi, A., Sadrnejad, S., *Discretization of Concrete Behavior into Four Planar Cases by Elastoplastic Multiplane Model*, International Journal of Civil Engineering, **5**, 1(2007), 48-65.

[35] Khosroshahi, A., Sadrnejad, S., *Substructure model for concrete behavior simulation under cyclic multiaxial loading*, International Journal of Engineering-Transactions A: Basics, **21**, 4(2008), 329.

[36] Rasoolan, I., Sadrnejad, S.A., Bagheri, A.R., *A geometrical inclusion-matrix model for concrete*, International Journal of Civil Engineering, **7**, 2(2009).

[37] Sadrnejad, S., Amiri, S.G., *A simple unconventional plasticity model within the multilaminate framework*, Int. Journal of Civil Engineering, **8**, 2(2010), 143-158.

[38] Chen, W.-F., Saleeb, A.F., *Constitutive Equations for Engineering Materials. Volume 1: Elasticity and Modeling*, Studies in Applied Mechanics, 37, 1994.

[39] Aghaei, A.A., Soroush, A., Reyhani, M., *Large-scale triaxial testing and numerical modeling of rounded and angular rockfill materials*, Scientia Iranica Journal, Transaction A: Civil Engineering, **17**, 3(2010), 169-183.

[40] Charles, J.A., *Strains developed in two rockfill dams during construction*, Géotechnique, 1975. **25**, 2(1975), 321-332.

[41] Materon, B., *Alto Anchicaya dam-Ten years performance*, in Concrete face rockfill dams-Design, construction, and performance, 1985, ASCE.

[42] Soroush, A., Araei, A. A., *Analysis of behaviour of a high rockfill dam*, Proceedings of the ICE-Geotechnical Engineering, **159**, 1(2006), 49-59.

[43] Alonso, E. et al., *Modelling the response of Lechago earth and rockfill dam*, GĂŠotechnique, **61**, 5(2011), 387-407.